SI Appendix

Table S1: Cloned sequences emerging from a Yeast-2-hybrid screen with StNRL1

Bait	No. of interacting clones	NCBI Top Potato protein match	NCBI Top Potato nucleotide match	Annotation
StNRL1	11/ 34	XP_006364807.1	XM_006364745.2	SWAP70 [*Solanum tuberosum*]
StNRL1	14/ 34	XP_006339816.1	XM_006339754.2	StNRL1 [*Solanum tuberosum*]
StNRL1	5/ 34	NP_001305469.1	NM_001318540.1	14-3-3 protein 1-like [*Solanum tuberosum*]
StNRL1	1/ 34	XP_006364862.1	XM_006364800.2	14-3-3 protein 7-like [*Solanum tuberosum*]
StNRL1	1/ 34	XP_002997507.1	XM_002997461.1	14-3-3 protein epsilon [*Phytophthora infestans* T30-4]
StNRL1	1/ 34	XP_006361409.1	XM_006361347.2	Protein phosphatase 2A regulatory subunit B"gamma-like [*Solanum tuberosum*]
StNRL1	1/ 34	XP_006367464.1	XM_006367402.2	Homeobox-leucine zipper protein HAT4-like [*Solanum tuberosum*]

Table S2. Primers used in this study.

Gene	Forward Primer	Reverse Primer	Function
StSWAP70	GW_StSWAP70F: AAAGCAGGCTTCACCATGGCTTCTAATGGAGCTC	GW_StSWAP70R: GAAAGCTGGGTCCTAAGGCTGATGAGAGTTA	gateway cloning of StSWAP70
NbSWAP70	SWAP70_V1F: CCCCGAATTCTCCAATGGATGACCTGACAA	SWAP70_V1R: CCCCGTTAACCTCCCTCAGCTTGGACTTTG	NbSWAP70 VIGS construct
NbSWAP70	SWAP70_V2F: CCCCGAATTCAGGCTGATGCCGAGACTAGA	SWAP70_V2R: CCCCGTTAACCCGCTGGACTGATGGTTAGT	NbSWAP70 VIGS construct
NbSWAP70	StSWAP70intF1: AAGGAAATCGAGGCAGCAAT		inter sequence primer
NbSWAP70	GW_StSWAP70F: AAAGCAGGCTTCACCATGGCTTCTAATGGAGCTC	GW_NbSWAP70R: GAAAGCTGGGTCCTAAGGCAGATGAGAGTTG	gateway cloning of NbSWAP70
NbSWAP70	qRT_NbSWAP70F: AAGCACATTTATGGCGTTCC	qRT_NbSWAP70R: TTCTTCTGCCCGAACAGC	qRT_PCR in *N. benthamiana*
StNRL1	StNRL_D28NF: CCTGCATTTACAGTTACATTACTGGGAATCTCTTGGGAG	StNRL_D28NR: CTCCCAAGAGATTCCCAGTAATGTAACTGTAAATGCAGG	StNRL1 mutant
StNRL1	StNRL_K42QF: TGAAACCAATGGGAACTGGTGCAGTGCAAAGGAGG	StNRL_K42QR: CCTCCTTTGCACTGCACCAGTTCCCATTGGTTTCA	StNRL1 mutant
Nb-ef1a	qRT_Nb-ef1aF:TGGACACAGGGACTTCATCA	qRT_Nb-ef1aR:CAAGGGTGAAAGCAAGCAAT	qRT_PCR in *N. benthamiana*
Pi02860	pDORNA-Pi02860-F: AAAAAGCAGGCTTCACCATGCTACCAACAAAC	pDORNA-Pi0286019-125-R: AGAAAGCTGGGTCCTAAAGATACTTGGTATA	Clone Pi02860 into gateway entry vector
Pi02860 Δ126-135	pDORNA-Pi02860-F: AAAAAGCAGGCTTCACCATGCTACCAACAAAC	pDORNA-Pi02860-10del R: AGAAAGCTGGGTCCTAAAGATACTTGGTATA	Clone Pi02860 Δ126-135 into gateway entry vector
Pi02860 Δ131-135	pDORNA-Pi02860-F: AAAAAGCAGGCTTCACCATGCTACCAACAAAC	pDORNA-Pi02860-5del R: AGAAAGCTGGGTCCTAAGCTTGAGGGTCTTT	Clone Pi02860Δ131-135 into gateway entry vector

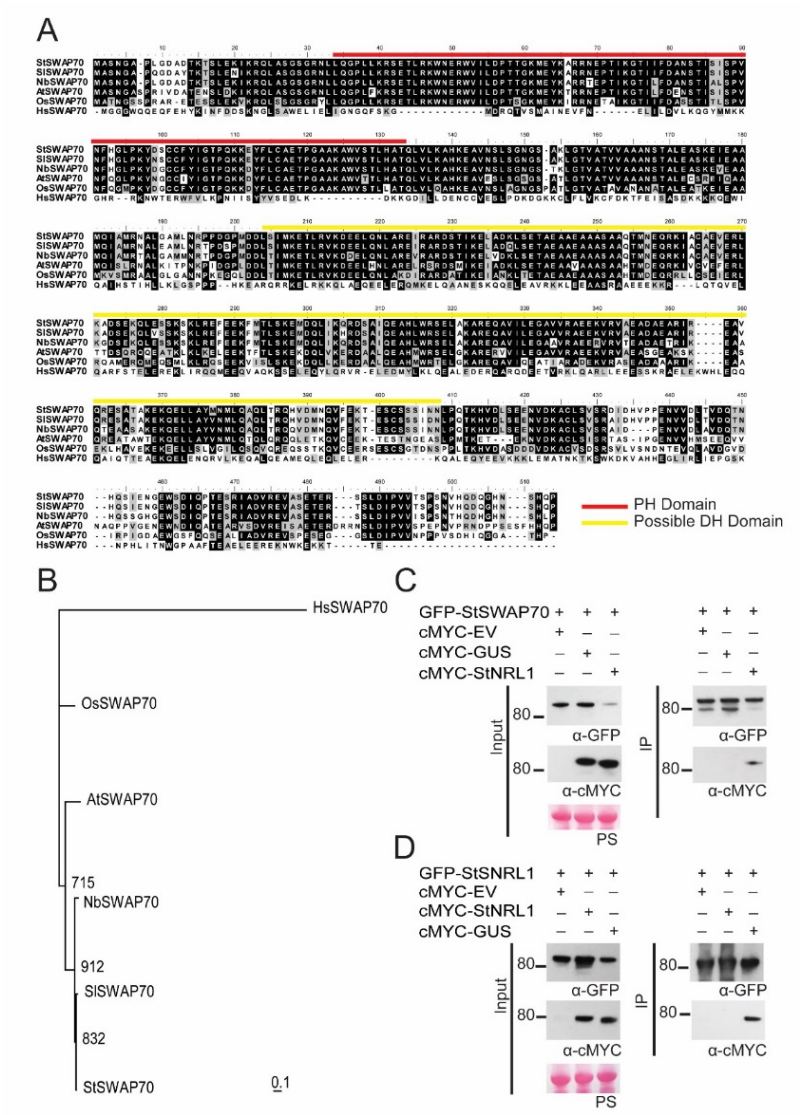

Fig. S1: Phylogenetic tree and alignment of SWAP70

A, Amino acid alignment of StSWAP70 and NbSWAP70 with the closest match in *S. lycopersicum*, SlSWAP70, Arabidopsis AtSWAP70 and *Oryza sativa* OsSWAP70 was generated in CLUSTALW. Conserved regions are coloured black. The red line shows the PH domain while the yellow line shows the possible DH domain.

B, Phylogenetic tree of SWAP70 sequences from *S. tuberosum*, *S. lycopersicum*, *N. benthamiana*, Arabidopsis, *Oryza sativa*, and Homo sapiens. A maximum likelihood tree was produced for the alignment using TOPALi v2.5 with 1000 bootstraps. The resulting tree was rendered with TreeView.

C, co-Immunoprecipitation (co-IP) assay using protein extracted from agroinfiltrated *N. benthamiana* leaves (replicating Fig 1C). cMYC-StNRL1-associated with GFP-StSWAP70, whereas cMyc-GUS did not. Expression of constructs in the leaves is indicated by +. Protein size markers are indicated in kDa, and protein loading is indicated by Ponceau stain (PS).

D, co-Immunoprecipitation (co-IP) assay using protein extracted from agroinfiltrated *N. benthamiana* leaves (replicating Fig 1D). cMYC-StNRL1-associated with GFP-StNRL1, whereas cMYC-GUS did not. Expression of constructs in the leaves is indicated by +. Protein size markers are indicated in kDa, and protein loading is indicated by Ponceau stain (PS).

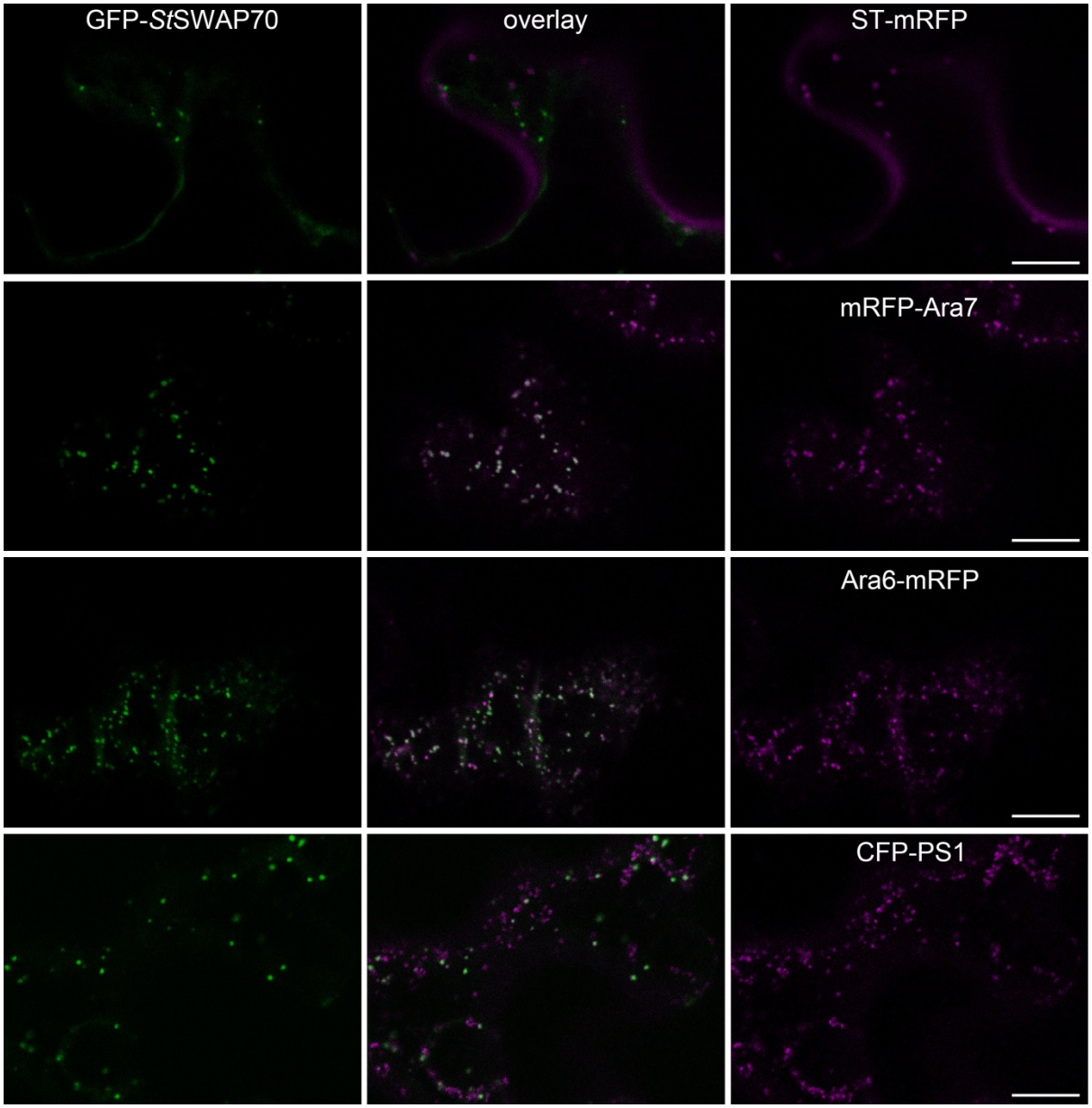

Fig. S2: StSWAP70 localises to endosomes with ARA7, ARA6 and PS1, but not to golgi.

Co-localisation studies using confocal laser scanning microscopy following transient co-expression (by agroinfiltration) in *N. benthamiana* of GFP-StSWAP70 and different subcellular markers: ST-mRFP (golgi), mRFP-Ara7, Ara6-mRFP, CFP-PS1 (blue PVC marker); Left picture shows GFP-StSWAP70 fluorescence, right picture shows marker fluorescence, and middle picture shows overlay of left and right pictures, all taken at 2 d after inoculation. Bars = 10 µm.

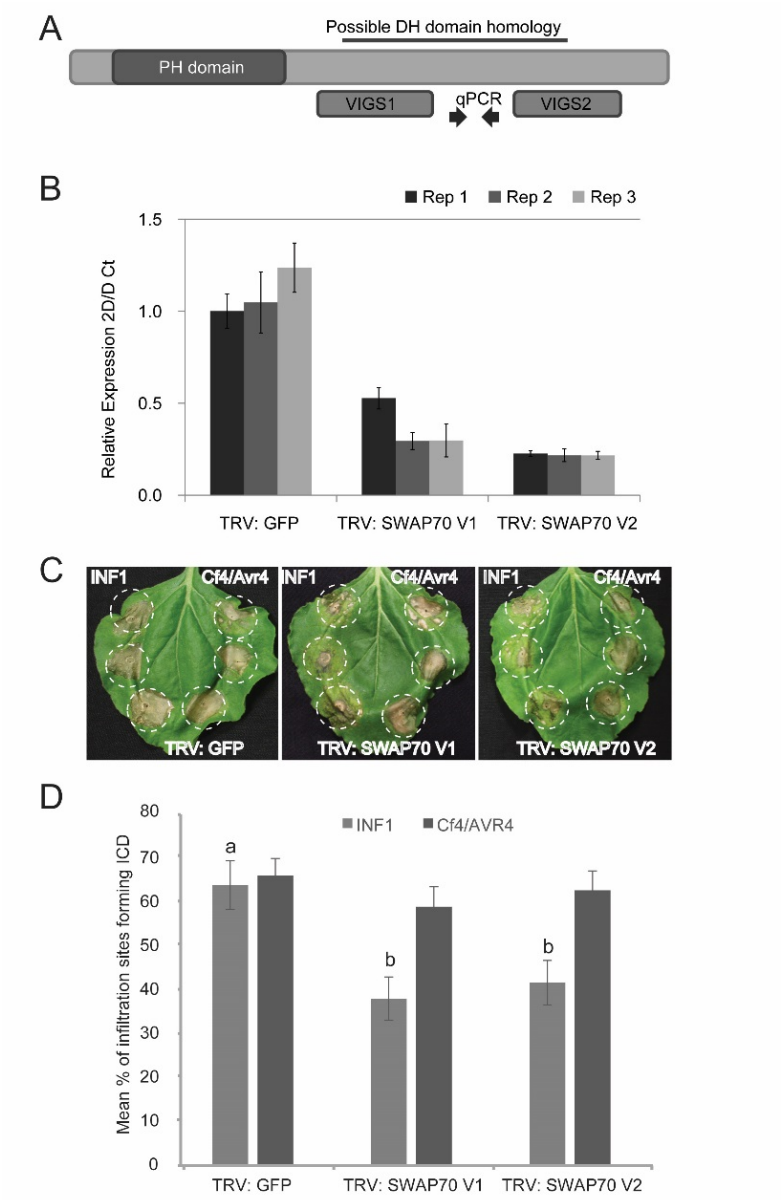

Fig. S3: Silencing *NbSWAP70* attenuates INF1-triggered cell death but not Cf4/Avr4.

A, Schematic diagram for the *NbSWAP70* gene with each domain shown along the top. The areas used to generate the VIGS silencing constructs and qRT-PCR primers are indicated below.

B, The graph shows the *NbSWAP70* mRNA levels detected by qRT-PCR in plants 3 weeks after agroinfiltration with TRV:GFP, TRV:SWAP70 V1 and TRV:SWAP70 V2 constructs. The analysis was performed using the 2Delta/Delta Ct method and the error bars indicate combined SE. Each column shows an individual biological replicate as indicated (Rep).

C, Representative leaf image showing the cell death of infiltration sites following over-expression of each construct with INF1 or Cf4/Avr4, as indicated, in *N. benthamiana* VIGS plants expressing TRV:GFP, TRV:SWAP70 V1 or TRV:SWAP70 V2.

D, Graph shows a significant decrease in ICD in TRV:SWAP70 V1 and TRV:SWAP70 V2 plants compared to the TRV:GFP control at 6 dpi. There is no significant difference of Cf4/Avr4 cell death on *NbSWAP70*-silenced plants compared to GFP control. Error bars are +/- SE and letters on the graph denote statistically significant differences (ANOVA, $P<0.001$; $n=55$).

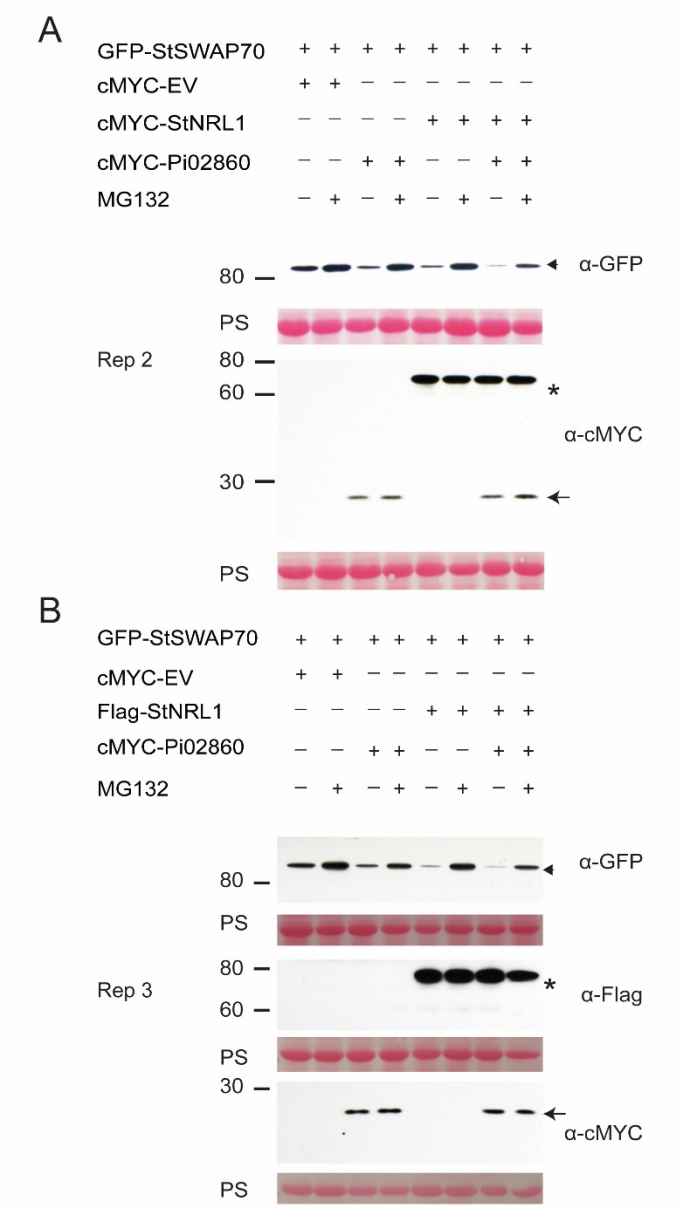

Fig. S4: Two additional replicates (as in Fig 3A) showing that co-expression of StSWAP70 with StNRL1 and/or Pi02860 causes proteasome-dependent degradation of StSWAP70

A, Co-expression of GFP-StSWAP70 with cMYC-StNRL1 and/or cMYC-Pi02860 causes proteasome-dependent StSWAP70 degradation, which is prevented by MG132 treatment. Transient expression of GFP-StSWAP70 alone, or co-expressed with cMYC-StNRL1 and/or cMYC-Pi02860 in *N. benthamiana* leaves, with or without treatment with MG132. Immunoblots with a GFP antibody showing protein fusions of GFP-StSWAP70 and the cMYC antibody shows protein fusions of cMYC-StNRL1 and cMYC-Pi02860 of the expected size.

B, An additional replicate of StSWAP70 degradation caused by co-expression of GFP-StSWAP70 with Flag-StNRL1 and/or cMYC-Pi02860. Expression of constructs in the leaves is indicated by +. Protein size markers are indicated in kDa, and protein loading is indicated by Ponceau stain. Immunoblots with anti-GFP shows protein fusion of GFP-StSWAP70 and the anti-Flag shows protein fusion of Flag-StNRL1 (star) and cMYC-Pi02860 (arrow) of the expected size.

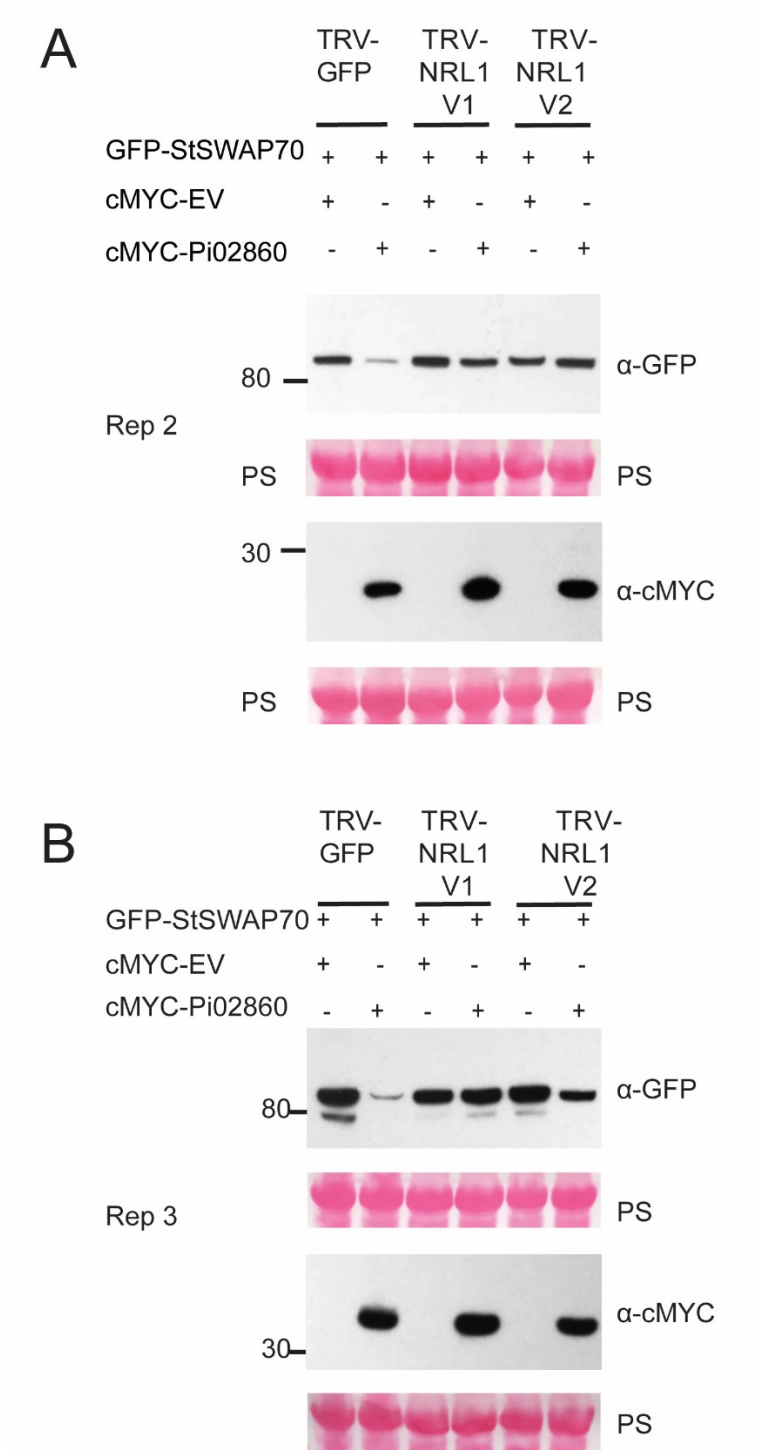

Fig. S5: Two additional replicates showing the attenuation of Pi02860-mediated degradation of StSWAP70 in *NRL1*-silenced *N. benthamiana* leaves compared to TRV-GFP (as in Figure 3B).

Expression of constructs in the leaves is indicated by +. Protein size markers are indicated in kDa, and protein loading is indicated by Ponceau stain. Immunoblots with GFP antibody shows protein fusion of GFP-StSWAP70 and the cMYC antibody shows protein fusion of cMYC-Pi02860 of the expected size.

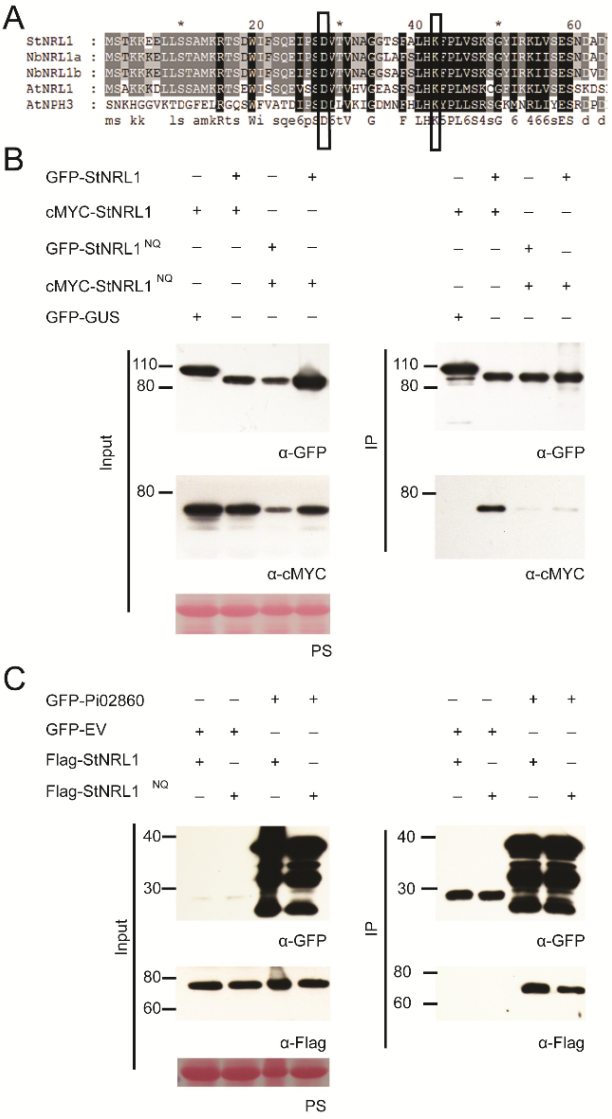

Fig. S6: The dimerisation mutant StNRL1^{NQ} shows reduced homodimerization but retains its interaction with Pi02860.

A, Multiple sequence alignment of the BTB domain in NRL1 homologous proteins. Conserved regions are highlighted in black. The two residues (D28 and K42) chosen to create StNRL1 dimerisation mutant StNRL1^{NQ} are indicated in the black boxes.

B, Immunoprecipitation (IP) of protein extracts from agroinfiltrated leaves using GFP-Trap confirmed that cMYC-StNRL1^{NQ} weakly associates with GFP-StNRL1^{NQ} or GFP-StNRL1 compared with a stronger association of wildtype cMYC-StNRL1 with GFP-StNRL1. cMYC-StNRL1 was not pulled down by GFP-GUS control. Expression of constructs in the leaves is indicated by +. Protein size markers are indicated in kDa, and protein loading is indicated by Ponceau stain. Immunoblots with GFP antibody shows protein fusion of GFP-StNRL1, GFP-StNRL1^{NQ}, or GFP-GUS and the cMYC antibody shows protein fusions cMYC-StNRL1 or cMYC-StNRL1^{NQ} of the expected size.

C, Co-Immunoprecipitation (IP) showing the association of GFP-PI02860 with both wild type FLAG-StNRL1 and dimerisation mutant FL:AG-StNRL1^{NQ} at similar levels. Expression of constructs in the leaves is indicated by +. Protein size markers are indicated in kDa, and protein loading is indicated by Ponceau stain. Immunoblots with GFP antibody shows protein fusion of GFP-Pi02860 and the FLAG antibody shows protein fusion of FLAG-StNRL1 or FLAG-StNRL1^{NQ} of the expected size.

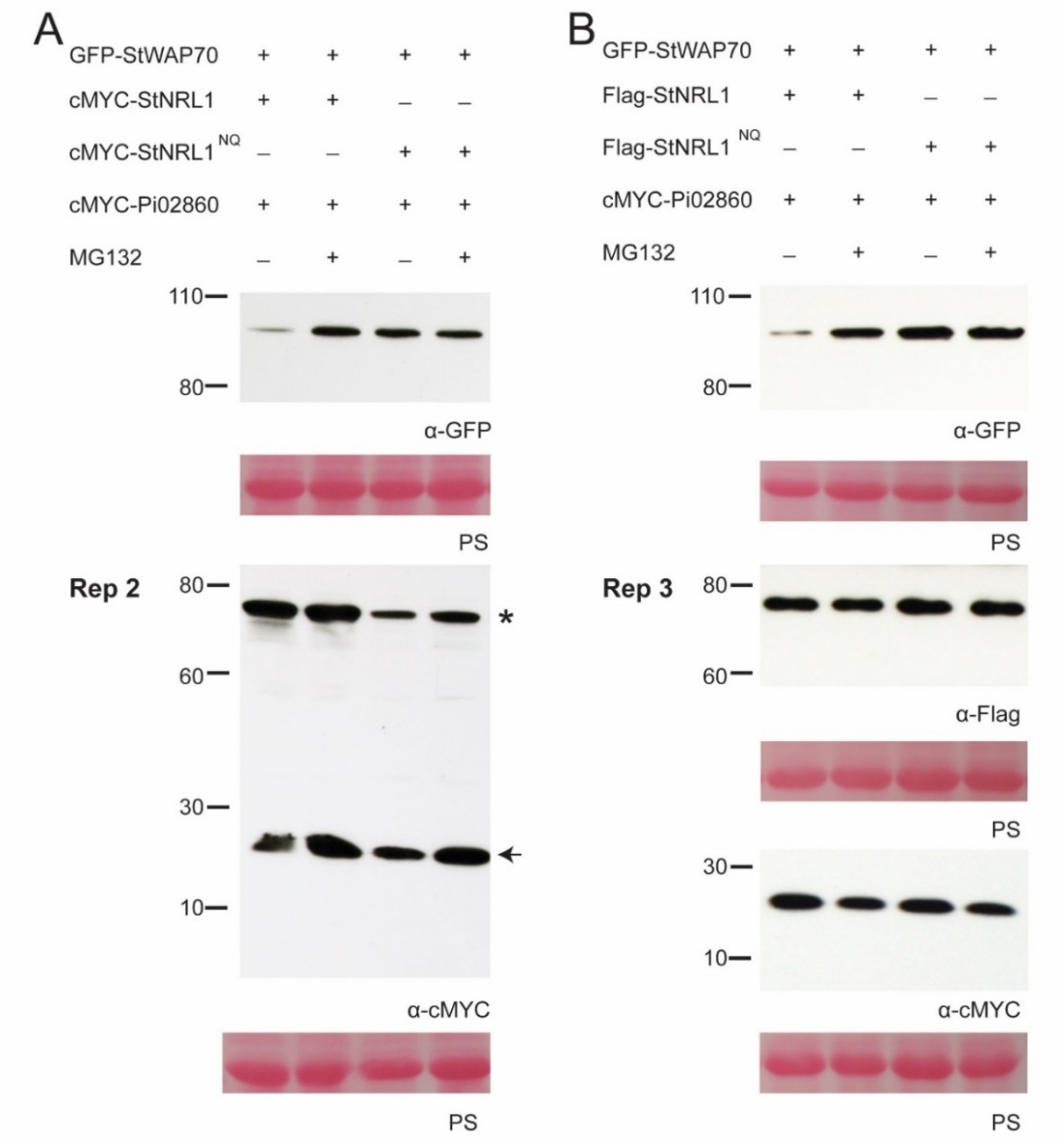

Fig. S7: Two additional replicates showing that the dimerization mutant StNRL1^{NQ} prevents degradation of StSWAP70 (As in Figure 4B)

A: Transient co-expression of GFP-StSWAP70 and cMYC-Pi02860 in the presence of either wild type cMYC-StNRL1 or mutant cMYC-StNRL1^{NQ} in *N. benthamiana* leaves, with or without MG132 treatment (Rep #2). Expression of constructs in the leaves is indicated by +. Protein size markers are indicated in kDa, and protein loading is indicated by Ponceau stain. Immunoblots with GFP antibody shows protein fusion of GFP-StSWAP70 and the cMYC antibody shows protein fusion of cMYC-StNRL1 or cMYC-StNRL1^{NQ} (labeled with start) and cMYC-Pi02860 (labeled with arrow) of the expected size.

B: Transient co-expression of GFP-StSWAP70 and cMYC-Pi02860 in the presence of either wild type FLAG-StNRL1 or mutant FLAG-StNRL1^{NQ} in *N. benthamiana* leaves, with or without MG132 treatment (Rep #3). Expression of constructs in the leaves is indicated by +. Protein size markers are indicated in kDa, and protein loading is indicated by Ponceau stain. Immunoblots with GFP antibody shows protein fusion of GFP-StSWAP70 and the Flag antibody shows protein fusion of FLAG-StNRL1 or FLAG-StNRL1^{NQ} and cMYC antibody shows protein fusion of cMYC-Pi02860 of the expected size.

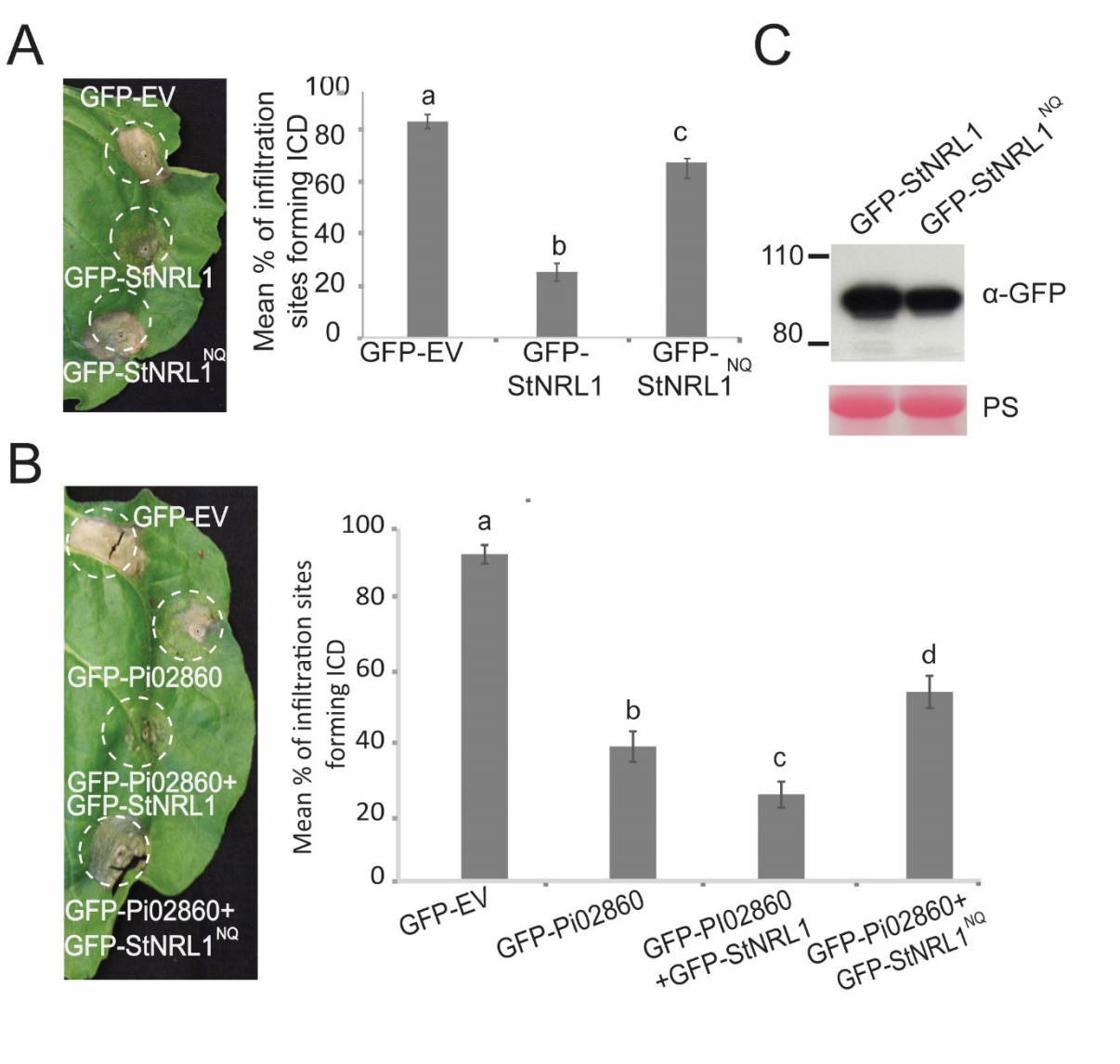

Fig. S8: StNRL1^{NQ} functions as a dominate-negative mutant that fails to enhance *P. infestans* colonisation.

A, Graph shows transient overexpression of GFP-StNRL1^{NQ} significantly (ANOVA, $p<0.001$, $n=104$) attenuates the suppression of ICD compared to GFP-StNRL1 wildtype in *N. benthamiana*. The results shown are combination of at least five individual biological replicates and error bars show +/- SE. Letters on the graph denote statistically significant differences. Representative leaf image show the cell death of infiltration sites following over-expression of each construct with INF1, as indicated.

B, Suppression of ICD by Pi02860 is significantly reduced ($p<0.001$, $n=89$) by co-expression with StNRL1^{NQ}. The graph shows the mean % of infiltration sites forming ICD by transient expression of INF1 with GFP-EV, GFP-Pi02860, GFP-Pi02860+GFP-StNRL1 or Pi02860+GFP-StNRL1^{NQ}. The graph represents the combined data from four biological replicates. Letters on the graph denote statistically significant differences. Representative leaf image (to the left) showing the cell death of infiltration sites following over-expression of each construct with INF1, as indicated, in *N. benthamiana*

C, Immunoblots showing stability of the StNRL1 and StNRL1^{NQ} GFP fusions. Western blotting indicates that the GFP-StNRL1 and GFP-StNRL1^{NQ} are similarly stable. Protein equal loading is indicated by Ponceau staining.

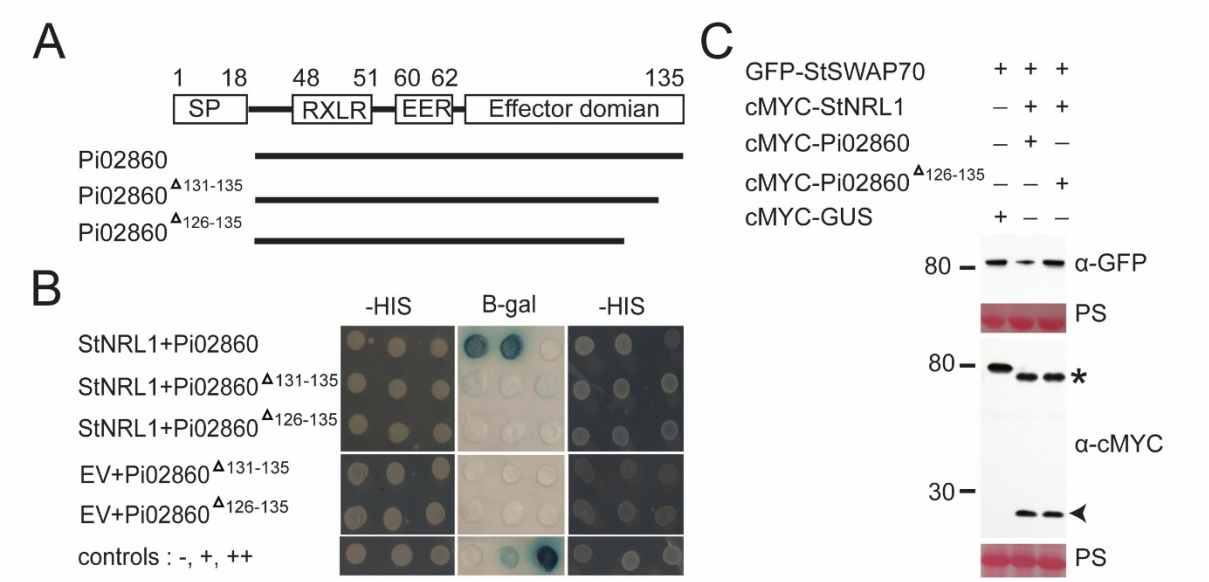

Fig. S9: The ten amino acid C-terminal deletion mutant Pi02860$^{\Delta 126-135}$ fails to degrade StSWAP70 when co-expressed with StNRL1

A, Schematic diagram for Pi02860 protein with each domain shown, with amino acid numbers at the top. The areas used to generate the Pi02860 ten (Pi02860$^{\Delta 126-135}$) and five (Pi02860$^{\Delta 131-135}$) amino acid deletion constructs are indicated below the wild type Pi02860.

B, Yeast co-expressing StNRL1 with Pi02860 grew on -histidine (-HIS) medium and yielded β-galactosidase (β-Gal) activity, whereas co-expressing StNRL1 with Pi02860$^{\Delta 126-135}$ did not, and only weak interaction was observed with Pi02860$^{\Delta 131-135}$. The +HIS control shows all yeast were able to grow in the presence of histidine.

C, A second replicate of the co-expression in Fig 5D showing the ten amino acid deletion in the C-terminal Pi02860$^{\Delta 126-135}$ fails to degrade StSWAP70 when co-expressed with StNRL1. Transient co-expression of GFP-StSWAP70 and cMYC-StNRL1 in the presence of wild type cMYC-Pi02860, deletion cMYC-Pi02860$^{\Delta 131-135}$ or cMYC-GUS control in *N. benthamiana* leaves. Immunoblots probed with anti-GFP show the protein fusion of GFP-StSWAP70, the anti-cMYC antibody shows protein fusion of cMYC-GUS, cMYC-Pi02860 and cMYC-Pi02860$^{\Delta 126-135}$ of the expected size.

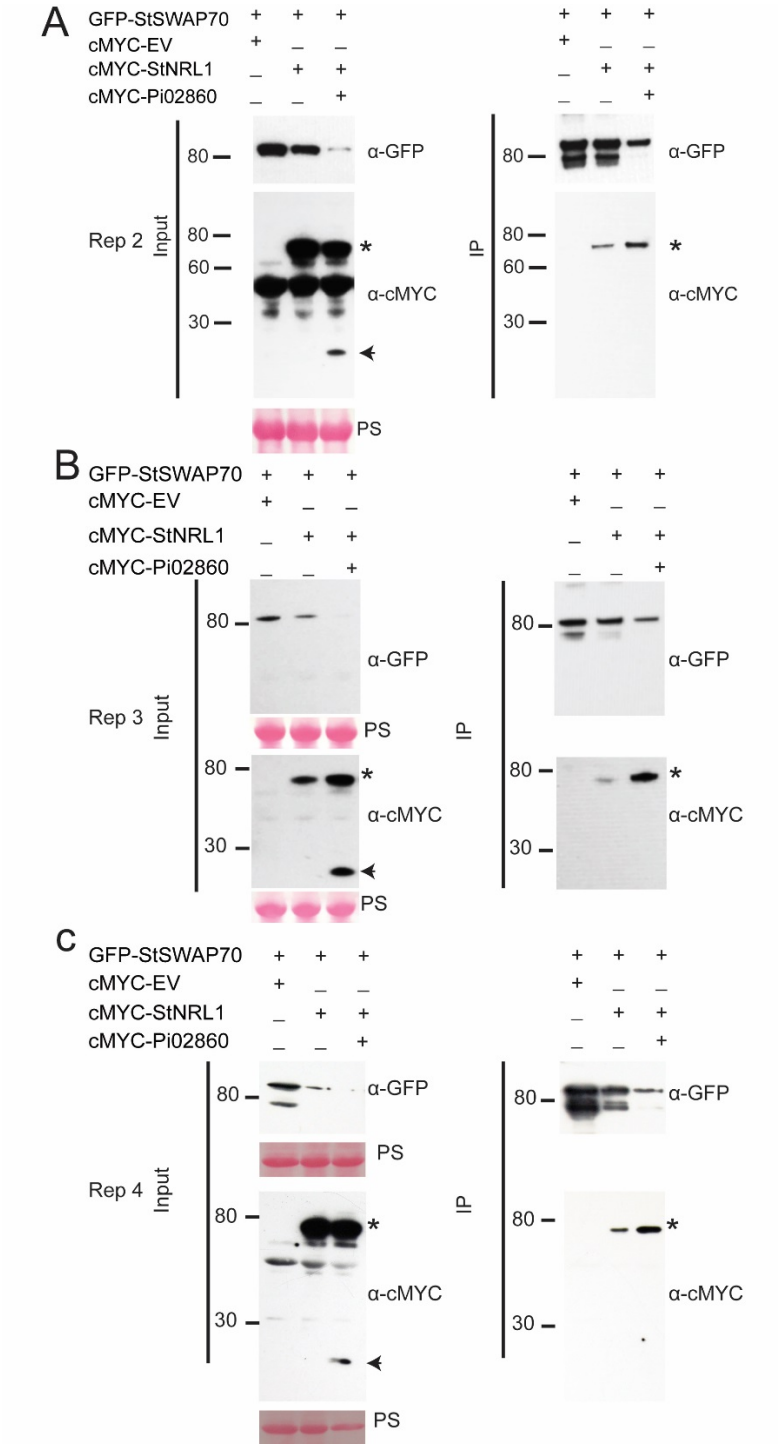

Fig. S10: Three additional replicates showing that Pi02860 enhances StNRL1 and StSWAP70 association *in planta* (as in Fig. 6)

A, B,C, Immunoprecipitation (IP) of protein extracts from agroinfiltrated leaves using GFP-Trap shows reduced protein levels of GFP-StSWAP70 in the presence of cMYC-StNRL1, which are further decreased when co-expressed with both cMyc-StNRL1 and cMyc-Pi02860. Increased cMYC-StNRL1 protein pull downs with GFP-StSWAP70 in the presence of cMYC-Pi02860 indicates that Pi02860 enhances the association between StSWAP70 and StNRL1.

Expression of constructs in the leaves is indicated by +. Protein size markers are indicated in kDa, and protein loading is indicated by Ponceau stain. Immunoblots with anti-GFP shows protein fusion of GFP-StSWAP70 and the anti-cMyc shows protein fusion of cMyc-StNRL1 (star) and cMyc-Pi02860 (arrow) of the expected size.